ISBN: 978-3-95450-223-3 ISSN: 2673-7000 doi:10.18429/JACoW-NAPAC2019-WEPLM60

FAST Sn-ION TRANSPORT ON Nb SURFACE FOR GENERATING Nb_xSn THIN FILMS AND XPS DEPTH PROFILING*

Z. Sun†, M. Liepe, J. T. Maniscalco, T. Oseroff, and R. D. Porter,
CLASSE, Cornell University, Ithaca, NY, USA
D. Zhang, Mechanical Engineering, Cornell University, Ithaca, NY, USA
X. Deng, Chemical Engineering, University of Virginia, Charlottesville, VA, USA

Abstract

In this work, we propose and demonstrate a fast and facile approach for Nb_xSn thin film deposition through the ion exchange reaction. By simply dipping a tin precursor on the Nb substrate surface, a ~600 nm thin film is generated due to the electronegativity difference between Sn and Nb. Through X-ray photoelectron spectroscopy (XPS) depth profiling, the compositional information as a function of film thickness was obtained. Results showed a Sn layer on the film surface, Sn-rich and Nb-rich Nb_xSn layers as the majority of the film, and a ~60 nm Nb_3Sn layer at the film/substrate interface. Quantitative analysis confirmed stoichiometric Nb/Sn ratio for the Nb_3Sn layer. This deposition method is demonstrated to be an alternative choice for Nb_3Sn film growth.

INTRODUCTION

Nb_3Sn thin film growth has drawn increased attention recently due to the potential of this material for replacing niobium (Nb) in superconducting radio frequency (SRF) cavities [1, 2]. Nb_3Sn can lead to superior RF performance owing to its high critical temperature (twice that of Nb) and also a higher superheating field. Considerable efforts have been made to explore Nb_3Sn film deposition on Nb substrate. The state-of-the-art approach relies on a tin (Sn) vapor diffusion process under >1000 °C high temperature in a high vacuum furnace [3]. Electroplating [4], sputtering [5], and chemical vapour deposition [6] are also actively being developed to coat Nb_3Sn-based cavities.

In this paper, we report an alternative method for generating Nb_xSn films based on fast Sn-ion transport on a Nb surface. Fast ion transport is a fast and facile approach which takes advantage of ion exchange reactions [7, 8]. As illustrated in Fig. 1a, the Nb-Sn alloy can be formed at room temperature when the Sn^{2+} cation containing organic electrolyte is exposed to a sufficiently polarized Nb surface. This fast reaction is enabled by the electronegativity difference between Nb and Sn [7]. Accordingly, the half reactions of Sn^{2+} reduction and Nb oxidation,

$$Sn^{2+} + 2e^- \rightarrow Sn\ (-0.14\ V), \qquad (1)$$

$$Nb \rightarrow Nb^{3+} + 3e^-\ (1.099\ V), \qquad (2)$$

yield a positive electrochemical potential, so the reaction

$$x\,Nb + Sn^{2+} + 2e^- \rightleftarrows Nb_xSn, \qquad (3)$$

is able to proceed spontaneously. Fig. 1b shows the grey-color Nb_xSn film from this Sn-ion transport process.

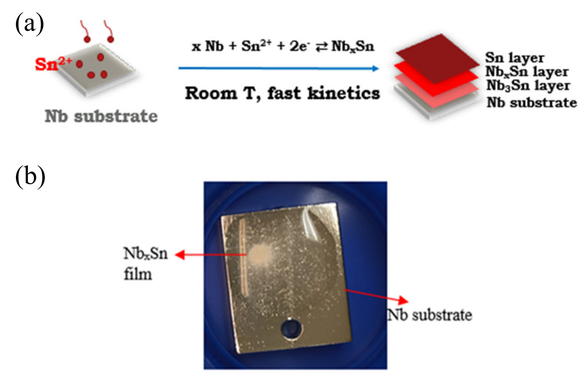

Figure 1: (a) Schematic showing the process of fast Sn-ion transport to the Nb surface. (b) Image of the generated Nb_xSn film on the Nb substrate.

In order to further improve the Nb_xSn film to a pure-stoichiometric Nb_3Sn film, the compositional characteristics are of great interest. The use of X-ray photoelectron spectroscopy (XPS) is specialized to characterize the composition at nano-scale (3-5 nm electron mean free path for Sn and Nb elements). By exploiting argon ion sputtering on the film surface and softly etching the film for a few nanometer, the depth profile of the film composition is analyzed in this study.

EXPERIMENTAL PROCEDURES

The Sn precursor, tin bis(trifluoromethanesulfonyl) imide (SnTFSI), was obtained from Alfa Aesar. 10 mM concentration solution was prepared by dissolving the precursor in DI water. 0.1 mL SnTFSI solution was dropped on the Nb substrate and then dried for 30 min. All these treatments were done in a glove box at room temperature. The film was observed immediately after the drying step.

XPS spectra were collected using a PHI Versaprobe III system with a sensitivity of < 0.1% atomic percentage. The system used monochromatic Al k-alpha X-rays with energy of 1486.6 eV and beam size of 200 µm. Ion sputtering was performed for 5.5 min in between each scan for data acquisition. In total, scans 1-35 were taken from the film surface to the film/substrate interface after each sputtering process. The etching rate of 3.6 nm/min was determined from standard SiO_2 films [9]. This work assumes the same sputter rate for Nb_xSn films. Thus, each scan probed the film with a step in depth of ~20 nm.

*This work was supported by the U.S. National Science Foundation under Award PHY-1549132, the Center for Bright Beams. Also, this work made use of the Cornell Center for Materials Research Shared Facilities which are supported through the NSF MRSEC program (DMR-1120296).
† zs253@cornell.edu

ISBN: 978-3-95450-223-3 ISSN: 2673-7000 doi:10.18429/JACoW-NAPAC2019-WEPLM60

The quantification is based on the integration of Nb 3d and Sn 3d peak areas. The effective atomic counts are affected by the relative sensitivity factor (RSF) between two elements, the electron mean free path (MFP, 1/3 of traveling distance for majority of collected photoelectron), and the transmission correction (T). The effective atomic counts for quantifying the Nb/Sn ratio are calculated by

$$Effective\ atomic\ counts = \frac{Peak\ area}{RSF * T * MFP}. \quad (4)$$

Additionally, the film surface was evaluated with a scanning electron microscope (SEM, Zeiss Gemini 500).

RESULTS AND DISCUSSION

Film Surface: Sn Layer

At the surface 80 nm-thin region, as shown in Fig. 2, XPS scans 1-5 observed identical shape and intensity for Nb 3d and Sn 3d peaks. The Sn peak intensity is prominent, while the Nb peak intensity is nearly zero, which suggests the film surface region is a Sn layer.

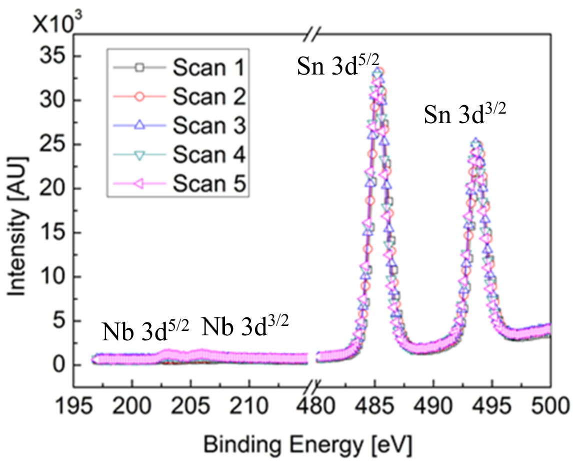

Figure 2: XPS depth profiling of film surface (Scans 1-5) showing a Sn layer.

Majority of the Film: Nb_xSn Layer

After probing the film beyond the 80 nm surface region, a ~420 nm thick Nb_xSn layer was detected at scans 6-28. Roughly, this Nb_xSn layer was divided into two roughly equal parts — a Sn-rich Nb_xSn region (scans 6-18) and a Nb-rich Nb_xSn region (scans 20-28).

As shown in Fig. 3a and 3b, the Nb intensity greatly increased along with the decrease of the Sn intensity from scan 6 to 18. However, the Nb/Sn ratio is still below 1.

Starting from scan 20, as shown in Fig. 3c, the Nb intensity became saturated. This saturation indicates that our measurement was not affected by the Nb substrate; otherwise, the Nb intensity would have continued to increase with the film being etched off from the substrate. The Sn intensity (Fig. 3d) continued to decrease, resulting in a Nb-rich Nb_xSn region where x is between 1 and 3.

Film/Substrate Interface: Nb_3Sn Layer

Further ion sputtering approached the interface between the film and substrate. The identification of this interface can be verified by observation of an increased Nb intensity after scan 34, where signal from the Nb substrate was significantly detected.

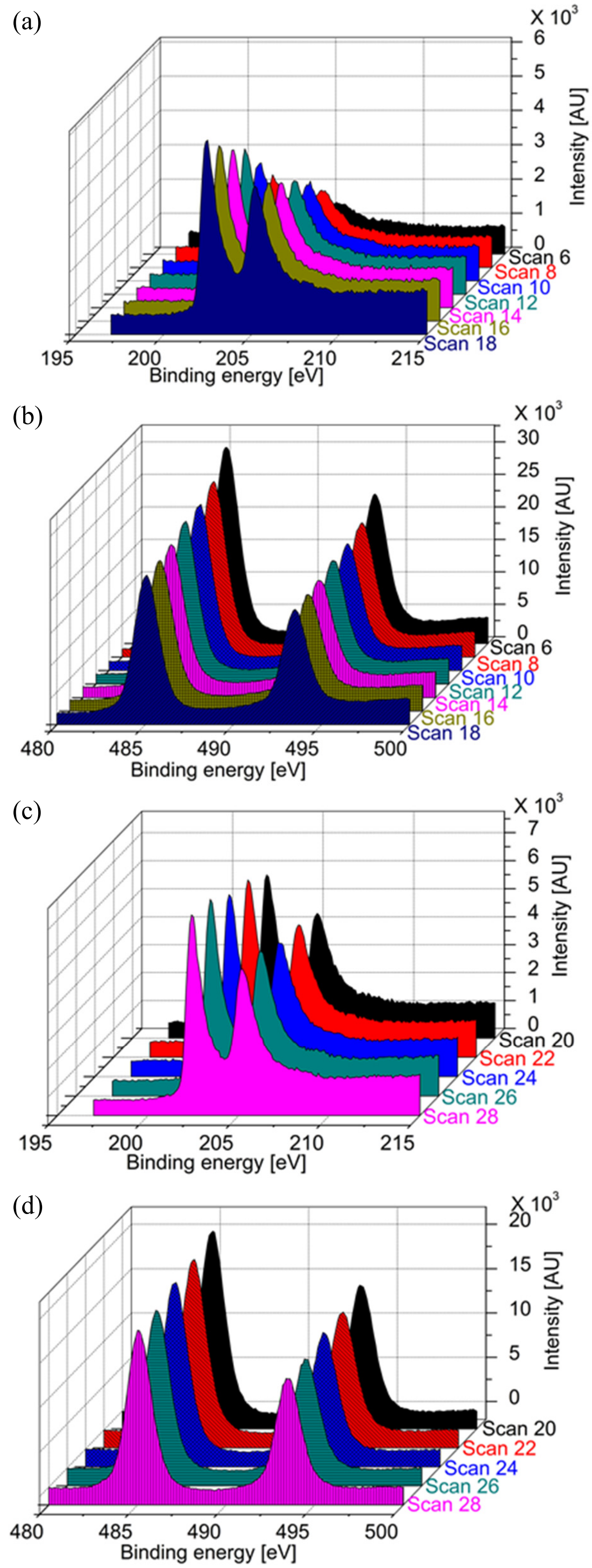

Figure 3: XPS depth profiling of majority of the film (Scans 6-28) showing the Nb_xSn layer. Sn-rich Nb_xSn layer (Scans 6-18): (a) Nb 3d, (b) Sn 3d. Nb-rich Nb_xSn layer (Scans 20-28): (c) Nb 3d, (d) Sn 3d.

ISBN: 978-3-95450-223-3 ISSN: 2673-7000 doi:10.18429/JACoW-NAPAC2019-WEPLM60

Table 1: Calculation of Nb/Sn Atomic Ratio at the Film/Substrate Interface

Element	Peak area	Relative sensitivity factor[10]	Mean free path[11]	Transmission correction[10]	Effective atomic counts	Atomic ratio
Nb	26330	8.21	3	400	2.67	2.93
Sn	49100	25.05	4.9	440	0.91	

We now focus on the spectra taken from the interface (scans 29-32). Figure 4 shows that the Nb and the Sn spectra of these scans are identical. More importantly, this 60 nm-thin region is stoichiometric Nb_3Sn. A detailed calculation of Nb/Sn compositional ratio for scan 31 is summarized in Table 1. The Nb 3d and Sn 3d characteristic peaks were first levelled using a straight background line. Their 3d peak areas were integrated without differentiating orbitals. The corresponding RSF values were obtained from the CasaXPS database. The RSF value for the Sn element is ~3 times higher than Nb, which greatly reduced the effective atomic counts from the Sn component. The resultant 2.93 ratio approximately matches with the composition ratio of Nb_3Sn.

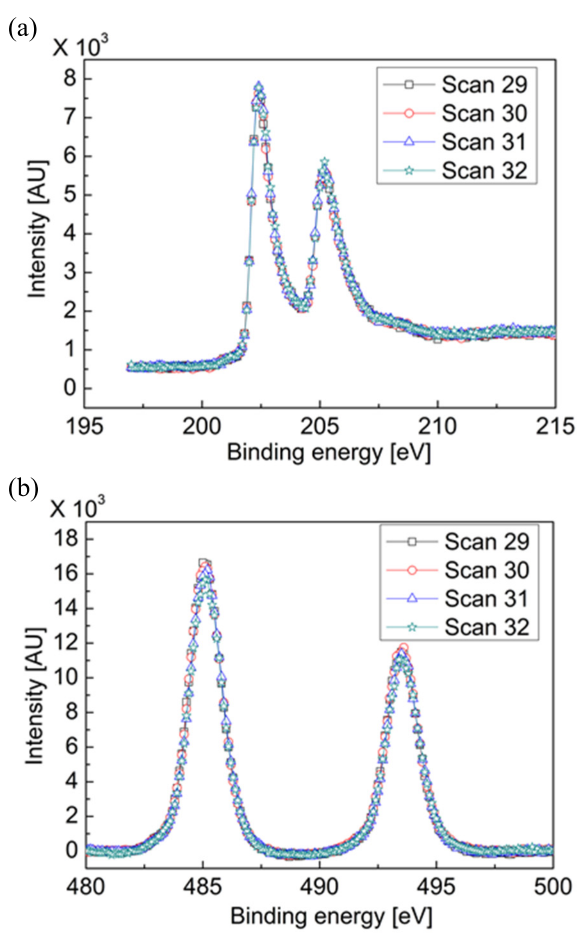

Figure 4: XPS depth profiling of the interface between the film and substrate (Scans 29-32) showing the Nb_3Sn layer: (a) Nb 3d, (b) Sn 3d.

Discussion

The 60 nm-thin Nb_3Sn layer is still smaller than the RF field penetration depth of ~170 nm for Nb_3Sn [2]. It is necessary to perform a heat treatment to improve the stoichiometry of the Nb_xSn layer and increase the thickness of the Nb_3Sn layer to >200 nm.

Also, the film surface, shown in the SEM image (Fig. 5), is less smooth than our electroplated Sn films [4]. Hence, after achieving required thickness of Nb_3Sn, a surface smoothing step would be beneficial since surface roughness is believed to be a critical issue impacting RF performance.

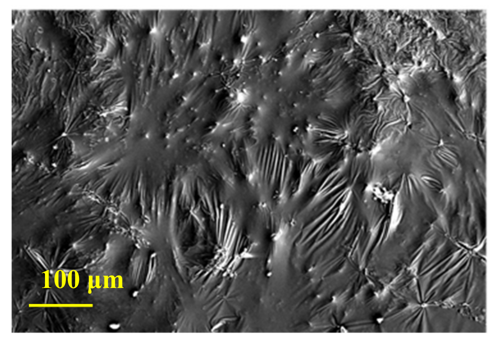

Figure 5: SEM image showing the film surface morphology.

CONCLUSIONS

In conclusion, a fast Sn-ion transport process was successfully developed to generate Nb_xSn films on Nb substrate. XPS depth profile revealed four regions from the film surface to the film/substrate interface: a ~80 nm Sn layer; a ~220 nm Sn-rich Nb_xSn layer; a ~200 nm Nb-rich Nb_xSn layer; and a ~60 nm Nb_3Sn layer. The stoichiometry of the Nb_3Sn layer was accurately quantified, and a Nb/Sn ratio of 2.93 was obtained. Further investigation is required to increase the thickness of the Nb_3Sn layer and reduce surface roughness.

REFERENCES

[1] S. Posen and D.L. Hall, “Nb_3Sn superconducting radiofrequency cavities: fabrication, results, properties, and prospects”, *Supercond. Sci. Technol.*, vol. 30, p. 033004, 2017.

[2] S. Posen, M. Liepe, and D.L. Hall, “Proof-of-principle demonstration of Nb_3Sn superconducting radio frequency cavities for high Q_0 applications”, *Appl. Phys.* Lett., vol. 106, p. 082601, 2018.

[3] S. Posen and M. Liepe, “Advances in development of Nb_3Sn superconducting radio-frequency cavities”, *Phys. Rev. ST Accel. Beams*, vol. 17, p. 112001, 2014.

ISBN: 978-3-95450-223-3 ISSN: 2673-7000 doi:10.18429/JACoW-NAPAC2019-WEPLM60

[4] Z. Sun *et al.*, "Electroplating of Sn Film on Nb Substrate for Generating Nb_3Sn Thin Films and Post Laser Annealing", presented at the 19th Int. Conf. RF Superconductivity (SRF'19), Dresden, Germany, Jun.-Jul. 2019, paper MOP014.

[5] E.A. Ilyina *et al.*, "Development of sputtered Nb_3Sn films on copper substrates for superconducting radio frequency applications", *Supercond. Sci. Technol.*, vol. 32, p. 035002, 2019.

[6] T. E. Oseroff *et al.*, "Performance of Samples With Novel SRF Materials and Growth Techniques", in *Proc. 9th Int. Particle Accelerator Conf. (IPAC'18)*, Vancouver, Canada, Apr.-May 2018, pp. 2475-2478. doi:10.18429/JACoW-IPAC2018-WEPMF047

[7] Z. Tu *et al.*, "Fast ion transport at solid–solid interfaces in hybrid battery anodes", *Nat. Energy*, vol. 3, p. 310, 2018.

[8] M. Winter and J. Besenhard, "Electrochemical lithiation of tin and tin-based intermetallics and composites", *Electrochimica Acta*, vol. 45, p. 31, 1999.

[9] Z. Sun, X. Deng *et al.*, "Silicon surface passivation by laser processing a sol−gel TiOx thin film", *ACS Appl. Energy Mater.*, vol. 1, p. 5474, 2018.

[10] CasaXPS database.

[11] R. Smart *et al.*, https://mmrc.caltech.edu/SS_XPS/XPS_PPT/XPS_Slides.pdf